IEEE Access
Multidisciplinary | Rapid Review | Open Access Journal

Received February 2, 2022, accepted February 12, 2022, date of publication February 15, 2022, date of current version March 10, 2022.

Digital Object Identifier 10.1109/ACCESS.2022.3151919

A New Technique Implemented in Synchronous Reference Frame for DVR Control Under Severe Sag and Swell Conditions

SAAD F. AL-GAHTANI[1], (Member, IEEE), ABDULWASA B. BARNAWI[1], HAITHAM ZAKI AZAZI[2], SHAIK M. IRSHAD[1], JAVED K. BHUTTO[1], MAJAHAR H. M.[1], AND ELBARBARY Z. M. SALEM[1,3]

[1]Electrical Engineering Department, College of Engineering, King Khalid University, Abha 61421, Saudi Arabia
[2]Electrical Engineering Department, Faculty of Engineering, Menoufia University, Shebeen El-Kom 32511, Egypt
[3]Department of Electrical Engineering, Faculty of Engineering, Kafrelsheikh University, Kafr El-Shaikh 33516, Egypt

Corresponding author: Haitham Zaki Azazi (haitham_azazi@yahoo.com)

This work was supported by the Deanship of Scientific Research, King Khalid University, under Grant RGP.1/255/42.

ABSTRACT Nowadays, power quality under the excessive implementation of power electronics devices is quite challenging issue. The compensation of non-sinusoidal; reactive and harmonic; components is the main role for power quality devices which highly depend on the robustness of the control system. Some common control systems are implemented using Synchronous Stationary Frame (DQ) theory. This paper proposes a new version of DQ control technique to control dynamic voltage restorer under severe transient voltage conditions. The power system network with the new DQ control technique is studied and analyzed under different scenarios to compensate for severe balanced and unbalanced voltage sags and swells. This new scheme is based on extraction of positive sequence components to implement the control algorithm. A mathematical model of the dynamic voltage restorer (DVR), hysteresis voltage control, converter controller model, new DQ scheme with complete system equations are carried out and verified using Simulink / MATLAB. The proposed system is validated experimentally using DSpace 1104 based laboratory system. The obtained results of the proposed compensation algorithm are compared with the results obtained from the traditional DQ method. Simulation and experimental results are correlated and show effectiveness of the proposed DQ control scheme.

INDEX TERMS Balance and unbalanced load, dynamic voltage restorer (DVR), instantaneous space vector, synchronous stationary frame (DQ) theory, voltage sag, voltage swell.

I. INTRODUCTION

Medical equipment, factory automation, semiconductor-device manufacturers, and paper mills are among the sensitive loads that are sensitive to power-supply disturbances [1], [2]. The increase in demand of high power quality and voltage stability becomes a progressively critical concern with serious threat and frequently occurring power-quality problem in today's power grids. voltage sag, swell are now recognized as severe costly consequences such as sensitive loads tripping and production loss [3]. Voltage sag and swell are significant power quality issues that occur frequently during contingency, switching and unexpected load changes [4]. Severe storms and lightning on electricity lines trigger line to ground fault leading to voltage sag over a wide section of electrical network. Some other factors that results in this disturbances are short circuits at the starting of power transmission line, the parallel power distribution line linked to the point of common coupling (PCC), high inrush currents related with the starting of large machines, abrupt changes in load, the energizing of power transformers, and switching operations in the power system network [5]. Voltage sag is the temporary drop of the root mean square (R.M.S.) voltage at a location in the electrical system below a predetermined threshold. It is a short-duration variation of the RMSvalue of voltage from 10 to 90% of nominal voltage over a time longer than 0.5 cycles (10ms) of power frequency but less than or equal to 60 seconds [6]. The terms used to define the extent of voltage sag are frequently misunderstood [7], [8]. According to IEEE 1159-2019, a sag to 70% is permitted,

The associate editor coordinating the review of this manuscript and approving it for publication was Ton Duc Do.

which indicates that the line voltage is dropped to 70% of its standard value, not dropped by 70%. A voltage dip of 70% will signify voltage reduced by 70% from the normal 100% voltage. The remaining voltage will be 30% or a sag to 30% [9]. The impacts of a sag are frequently more perceptible than the effects of a swell. A sag with more than three cycles is frequently observable as a reduction in voltage output. Sags are frequently unrecognizable from brief outages because the effects on the equipment are similar [2], [10], [11]. Computers and other sensitive equipment may encounter unexpected shutdowns or distorted voltage waveform [6]. Even motor starter relays and contactors can be hypersensitive to voltage sags, resulting in process shutdown when the drop out occurs. For over 1000 cycles, a wide disparity has been discovered, varying from 20% to 65% sags [12].

Swells are due to large loads shutting down, quick changes in load resistivity, and other factors. A voltage swell is an electromagnetic disturbance that occurs in two dimensions [12], [13]. When a voltage swell occurs, the RMS voltage will increase temporarily at a point above a specified level. Both voltage level and length of duration influence the voltage swell; the voltage swell's start threshold is 110 percent, and the length ranges from 0.5 cycles (10ms) to 60 seconds. The repercussions of a swell are frequently more damaging than that of a sag. The overvoltage issue results in malfunctions of the power supply equipment, though the effect may be gradual and cumulative. If the duration is longer than three cycles, the increase in output in a voltage may be noticeable [7].

When the industries were using solid state devices, there was no much importance for the quality of the supplied voltage. But when the industries replace the solid-state devices with the power electronic devices, the quality of the voltage supplied became the most important aspect [14], [15]. The short scale solutions available for voltage sag and swell are using a universal power supply (85V-264V), using Semiconductor Equipment and Materials International (SEMI F47) compliance power supply, adjusting the trip threshold, reprogramming the response of adjustable speed drives (ASD), using reverse powered relays, single phase power conditioners, uninterrupted power supplies, constant voltage transformers, drip proofing inverters etc. The large scale solutions available are using three phase power conditioners, three phase uninterrupted power supplies, active voltage conditioners, data wave, fly wheel, dynamic voltage restorer (DVR) etc [9].

Several power electronic devices have been developed to improve voltage stability and overcome the harmful impacts of voltage sag/ swell. DVR is an effective component for compensation of voltage disturbance that is commonly utilized in practice [16]–[18]. Among the power electronics devices, DVR is a switching device that induces synchronous voltage and can be thought of as a series active power filter. To have an economic and efficient power supply, DVR is used. It's a power electronic FACTS device used for compensation of voltage sags and swells in electrical power distribution [19]. The first DVR system with static VAR devices, which was installed in 1996 in Anderson, South Carolina, was a 12.47 kV system.

DVR help in resolving problems of a power system that has voltage disturbances. it is an active inverter that adjusts the voltage, either through a transformer or without a transformer in series and in synchronization with the grid at the PCC [20], [21]. Calculation of the compensation voltage is done by comparing the reference load voltage and the actual voltage of the grid. under a voltage sag or swell, the controller identifies the magnitude and phase of the compensated voltage required. the generated reference voltages are sent to the modulator to generate the switching pulses. These pulses would shoot the DVR switches, and the voltage from the DVR would be injected into the PCC to substitute for the voltage disturbances. Therefore, DVR can be considered or presumed as a filter that separates the grid from the load and compensate for any voltage sag or swell. Thus, the end user would not be able to sense or get effected with the problem of voltage disturbance induced by the utility [4].

The main concern in utilizing DVR is the efficient control of DVR when injecting real and reactive power [22]. In a DVR, the main functions of the control system are to identify the voltage drops or swells, to generated voltage reference signal, controlling converter and the protection of the system [21], [23]. The quality and accuracy of the detection methods will have a big impact on the performance of the control algorithm. For example, the detection algorithms like Discrete Fourier Transform (DFT), Fast Fourier Transform (FFT), and Kalman filtering (KF) are used to accurately predict voltage disturbances in the supply voltage [23], [24]. These algorithms are called detection algorithms. The KF is a decent way to figure out which sags are balanced and unbalanced. Clark's transformation and Park's transformation are used by the Synchronous Rotating Frame (SRF) to identify sag and swell [25]. The Park's transformation or DQ transform can only be used to figure out balanced three phase sags. The multiple DQ transform is a different method that can be used for harmonics and unbalanced sag conditions. Multiple DQ transform was made easier by having separate modules for retrieving positive and negative sequence components from fundamental and harmonic waves [26], [27]. Though easy extraction of sequence components, this methodology is incompatible for single phase system, fails to identify the unbalance sag and swell voltages and it has complex procedure to get the reference voltage to control the DVR. The DQ has advantage of short duration for detection of sag/swell in a three-phase system.

This paper proposes a modified DQ method for DVR control. The proposed detection technique is based on a time-domain algorithm for identifying positive sequence component of grid voltage. This DQ method rely on detection technique of sequence components which doesn't constitute both adaptive mechanism (like PI controller) and signal filtering [26], [28]. This provides less computational time leading to fast response of the control system with decent stability and wide range of operating conditions including extreme

sags and swells. Unlike other method, the proposed method is compatible for both balanced and unbalanced systems. In addition, this control method achieves almost zero tracking error in all abnormal-operating conditions. The control system is mathematically represented and verified in simulation as well as experimentally validated. Finally, the proposed control is compared to the traditional DQ method to confirm the superiority of the proposed method.

The paper is organized in the sections as followed. Section II provides discussion on DVR. Section III describes the proposed DQ algorithm. The experimental setup is described in Section IV. Section. The result illustration as well as a discussion is presented in section V. The performance of the proposed DVR control system is summarized in Section VI.

II. DYNAMIC VOLTAGE RESTORER (DVR)

To restore the load side voltage to the desired amplitude and waveform, injection of compensation voltage with desired magnitude and frequency is necessary [16]. The system can inject up to 50% of nominal voltage, but only for a short time (up to 0.1 second). However, most voltage sags are much less than 50 percent. This is said to be Dynamic voltage restoration or regulation. The regulating device is said to be DVR [29]. DVRs may provide good solutions for end-users subject to unwanted power quality disturbances [30]. Figure 1 shows a basic DVR power system circuit supported with control circuit to inject compensated voltage for maintaining the voltage at desired value [24], [31]. DVRs usually installed on a critical feeder supplying the active power through DC energy storage and the required reactive power is generated internally [4].

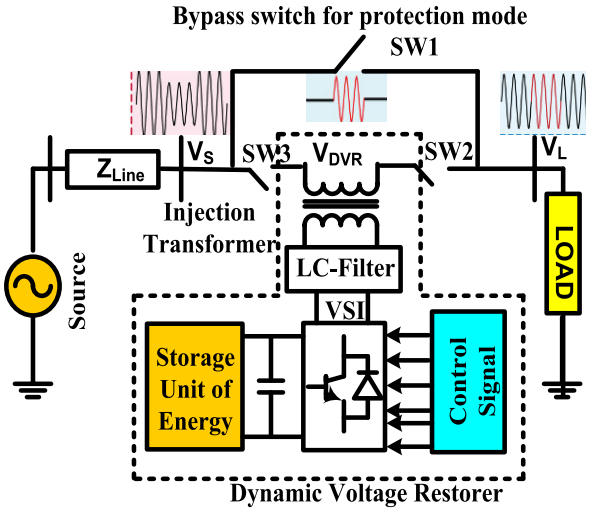

FIGURE 1. Basic circuit of power system with DVR.

A. OPERATION MODES OF DVR

Based on the functioning, a DVR modes of operation are divided in to three modes, which are, Protection, Standby and voltage injection [21], [32]. In protection mode, exceeding the load current over permissible value due the short circuit or large inrush current, DVR will be isolated from the power system using switches, SW_2 and SW_3 as shown in Figure 1 and thus providing an alternative path for the load current flow through SW_1 [32], [13].

In standby mode, the low voltage winding of the booster transformer is shorted by the converter and full load current is passed through the primary of the booster transformer. In this mode of operation, the DVR will not inject any compensation voltage into the power system network.

This mode of operation is initiated when a disturbance in voltage is detected and ends when the voltage is recovered to its normal operating condition.

B. COMPENSATION METHODS

Voltage compensation methods are selected based on the DVR power rate, load types, situations, fault types and so on [14]. The compensation methods are divided into pre-sag, in-phase, and energy minimized. In pre-sag, the controller monitors the supply voltage and identify any voltage fluctuations, then generates and injects the difference of voltage. As a result, the load voltage remains unchanged as the pre-sag voltage.

In-phase compensation approach, the injected voltage and voltage of supply are in phase with each another [33]. This approach is not suitable for sensitive loads as phase shift occur during most voltage sag scenarios. On the other hand, it is suitable for linear loads when the voltage magnitude is significant.

The main drawback of the pre-sag and in-phase methods is to provide real power at the DC-link. This can be overcome by Energy-minimised (EM) method, as the exchange of active power is not carried out during the compensation stage. It can be stated specially for sag mitigation that real power is neither injected into the network or absorbed from the power supply [21].

C. DVR CONTROL TYPES

DVR control schemes are divided into two categories: linear and nonlinear [35].

When working with static power converters, linear control is usually used as the conventional method. This control is widely used in the power quality systems such as to implement compensation of voltage or current disturbances, to protect critical equipment from failing, to reduce financial loss [36], [37]. Medical and industrial systems that are sensitive and important should be protected in a reliable and cost-effective manner.

Nonlinear controllers are more appropriate than linear controllers. One significant disadvantage of the nonlinear controller is that derivative operations can create issues with electromagnetic interference on inverter switching, resulting in substantial control errors. actually, a high pass filter can be used to substitute the derivative behavior, which improves

performance while attenuating high frequency noise in sensors and cables [35], [38].

D. CONTROL STRATEGIES AND ALGORITHMS OF DVR

The detection of voltage disturbances is the major emphasis of the DVR's control system. Specifically with sensitive loads, the detecting system should be fast enough to identify the voltage disturbance accurately for assessment of DVR performance [22]–[23]. As shown in Figure 2, various methods for voltage disturbance detection have been proposed, including RMS, Peak Value, DFT, Fourier Transform (FT), Wavelet Transform (WT), Windowed Fast FT (WFFT), ABC to DQ axis transformation, KF, Phase-Locked Loop (PLL), and SRF [39], [41]. The benefits and drawbacks of the most serious voltage disturbance detection techniques are provided in Table 1.

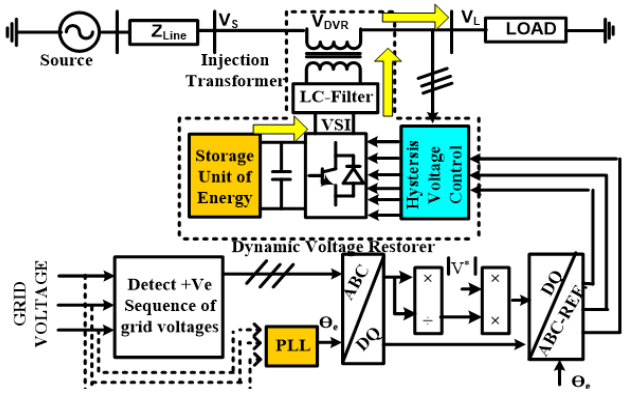

FIGURE 2. Schematic diagram of the proposed system with DVR.

E. PROPOSED SYSTEM DESCRIPTION

The proposed configuration shown in Figure 3 includes a supply (grid) voltage with grid impedance, a three-phase load, an injection transformer, and the DVR system. The DVR system comprises of a Voltage Source Inverter (VSI) powered by a DC power source with a dc link capacitor, and a harmonic passive filter. A three-phase balanced, and unbalanced load is considered in this system [39], [41].

1) ENERGY STORAGE UNIT AND DC-LINK CAPACITOR

The energy storage system (ESS) and the dc link capacitor are two essential components in a DVR system that supplies the active power required to protect against prolonged disruptions. The dc link capacitor is an energy storage device that generates high-power short-time pulses to offer dynamic response [12], [22]. A DVR's ESS is generally made up of a battery. Table 2 illustrates the energy and power density of typical capacitors and batteries, as well as their life cycle count and discharge times.

A battery and a capacitor can be used together to meet the energy requirements of a DVR, as indicated in Table 2. The application determines the size of an energy storage

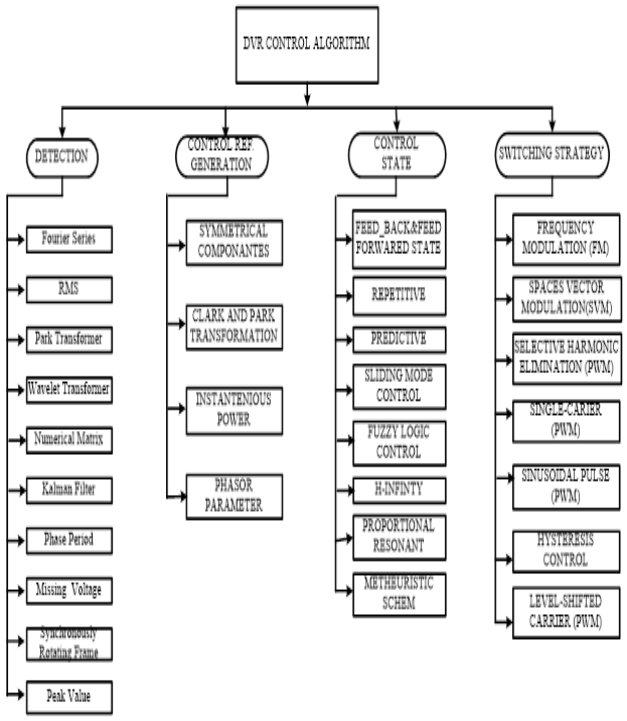

FIGURE 3. Flow chart for control strategies of DVR.

device [45]. The average energy storage requirements for power grid levelling, power quality, and specialized appliances are presented in Table 3. A DVR system's energy storage capacity must be sufficient to fulfil the power quality and custom device requirements for a few seconds and cycles, respectively [37], [45].

The energy stored in a capacitor is given in the following equation as a function of capacitance and voltage.

$$E = \frac{1}{2}Q * V(J) \quad E = \frac{1}{2}C * V^2(J) \tag{1}$$

The capacitance of the dc link was calculated as follow.

$$E = \frac{2 * E}{V^2}(J) \tag{2}$$

2) LC FILTER DESIGN

To decrease harmonics caused by the pulse with modulation (PWM) voltage waveform, the output side of the DVR's inverter is connected to an LC filter. The cutoff frequency for an LC filter is designed to eliminate the output voltage waveform's lowest order harmonics [46]. The cutoff frequency or resonant frequency is dependent on the filter capacitance and inductance, as presented in equation (4) [47]. The capacitor value should be chosen so that the resonant frequency is less than one-third of the switching frequency of the inverter

$$\omega_n = \frac{1}{\sqrt{L_{LPF}C_{LPF}}}\left(\frac{rad}{sec}\right) \tag{3}$$

$$f_n = \frac{\omega_n}{2\pi} = \frac{1}{2\pi\sqrt{L_{LPF}C_{LPF}}}(Hz) \tag{4}$$

TABLE 1. Voltage disturbance detection techniques benefits and weakness.

Detection Method	Benefits	Weaknesses
Peak Value [42]	0.25 cycle delay in identifying sags/swells.	Pass over noise, difficult to extract phase angle
Discrete Fourier [43]	Sags/swells recognition, harmonic distortion	Requires stationary signal, high Calculations (one cycle for perfect sag/swell value and phase data),
Root Mean Square[6]	Identifies start-/end- of sags/swells, simple, fast	Fails to detect the frequency, harmonic, and phase angle
Fast Fourier Transformation [44]	Quicker than DFT, identifies phase angle shifts, harmonic distortion, precision	Requires stationary signal, integer sample numbers
Phase Locked Loop[41]	Sags/swells recognition, phase angle	Requires time delay upward half-cycle, difficult to control
Synchronously Rotating Frame [34]	Fit for three-phase Very short time for detection	incompatible for single-phase systems, fails to Identify the imbalance of sags/swells voltage
Wavelet Transform[43]	Ease of use time and frequency data	Requires accurate choice of wavelet model, need a delay associated to wavelet models
Kalman Filter [6]	Ideal recognition of voltage sags/swells, solid for working with linear structures	Requests enhanced KF for non-linear structures

TABLE 2. Difference between capacitor and batteries.

Apparatus	Energy Intensity (Wh/Litter)	Power Intensity Watt/Litter	(Cycle Life count)	Discharge Time (Sec)
Capacitor	0.04 -5	(0.1-1000) *106	(0.1-1)*106	<1.01
Batteries	55-255	155	(0.001-1)*103	>999

TABLE 3. Stored energy capability requests by applications.

Application	Stored Capability	Discharge time
Custom Appliances	(11 – 1100) 104J	Few Cyc.
Power Quality	(11 – 1100) 104J	Few Second
Power grid Turning	(11 – 201000) MJ	Few Sec. – Few days

3) INJECTING TRANSFORMER

The DVR uses three single-phase injection transformers, as shown in Figure 4, to inject the three phase voltages created by the voltage source inverter [45]. To maximize the output voltages produced by the inverter, the secondary side (low voltage side) of each transformer is coupled in a wye arrangement [45].

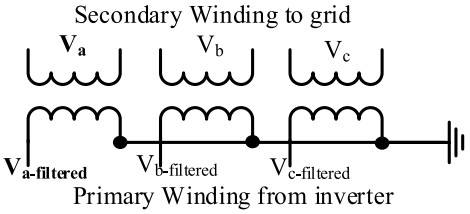

FIGURE 4. Injecting transformer.

The following important factors has to be considered while designing the injection transformer [13].

4) DC VOLTAGE COMPONENT DESIGN

A proper selection between the air gap and the magnetizing current is required for an efficient injecting transformer [10], [45]. When the DC voltage V_0 is applied across the primary of the injecting transformer, dc current I_0 will flow through the primary winding N_p leading to the dc flux circulating in the core, resulting in a dc flux density B_{dc}. This dc flux density is evaluated by following

$$B_{dc} = \frac{0.4\pi N_p I_0}{I_g + \left(\frac{l_m}{\mu_m}\right)} \tag{5}$$

where l_m and μ_m are mean length of the core and permeability of the core respectively. Practically this dc flux is complemented by the ac flux B_{ac_max} and is evaluated as

$$B_{ac\_max} = \frac{V}{KfA_cN_p} \tag{6}$$

where V is the RMS value of the supply voltage, K is the coefficient of the wave form, f is the fundamental frequency of the supply voltage and A_c is the cross-sectional area of the core of the transformer. The sum of the dc flux density (B_{dc}) and ac maximum flux density (B_{ac_max}) should be less than the rated maximum flux density of the core B_{max} as

$$B_{dc} + B_{ac\_max} < B_{max} \tag{7}$$

If the above condition is violated then the transformer may reach to the saturation condition.

5) CALCULATION OF RATED AC VOLTAGE

The voltage applied to the primary of the DVR transformer is combination of voltages at different frequencies [24], [48]. The sum of the maximum flux densities (at the different frequency components) should be less than the permissible maximum value of the ac flux density $B_{ac\_max\_eqa}$ and is given by

$$B_{ac\_max\_equ} = B_{1max}\cos(\omega t + \delta_1) + B_{2max} \times \cos(2\omega t + \delta_2)\ldots B_{nmax}\cos(n\omega t + \delta_n) \tag{8}$$

where $B_{1max}, B_{2max} \ldots B_{nmax}$ are the maximum flux densities of voltages at multiple frequency components x = 1, 2 . . . n respectively.

The maximum flux density at the fundamental frequency voltage component is given by

$$B_{1max} = \frac{|V_1| X10^4}{KfA_cN_pf_1} \tag{9}$$

Similarly at different frequencies of $f_2, f_3, \ldots f_{fn}$ the maximum flux densities $B_{2max}, B_{3max} \ldots .B_{nmax}$ can be evaluated. At every half cycle of the least frequency value, flux density reaches its maximum and this value mostly depends on the least frequency component. Therefore, fundamental frequency is opted and the equivalent voltage is can be expressed by substituting fh = hf1. Then the equation above is changed to

$$B_{hmax} = \frac{\left(\frac{|V_1|}{h}\right) X10^4}{KfA_cN_pf_1} \tag{10}$$

where h = 2, 3, . . . n. it can be observed that the B_{hmax} is the function of fundamental frequency. Design of the injecting transformer considering all the frequency component is a very complex and hectic. Hence equivalent fundamental component is evaluated by considering all components with the followin

$$B_{ac\_max\_eqa} = \frac{|V_{1equ}| X10^4}{KfA_cN_pf_1} \tag{11}$$

By substituting equation (10-12) in equation (9) we can calculate the RMS voltage for the injecting transformer represented by

$$V_{1equ} = |V_1| + \sum_{h=2}^{n} \frac{|V_h|}{h} \tag{12}$$

where V_{1equ} is the primary voltage referred to the secondary of the injecting transformer.

The above discussion suggests DVR has many parameters like DVR components, design parameters and different control methods that has to be perfectly opted while designing DVR system.

III. NEW DQ ALGORITHM

In abnormal operating conditions, symmetrical components (positive and negative sequence components) appear in the system voltages affecting the load voltages. Based on the appearance of negative sequence components, the proposed control system is intended to separate the positive sequence components from the system voltage by the proposed detection technique. These positive sequence components are transformed into dq coordinates to generate the reference of load voltages. The reference voltages are compared to the actual load voltages to generate firing signals of voltage source inverter (VSI) switches using Hysteresis voltage control [49].

This proposed detection technique allows instantaneous and continuous detection of positive sequence components and compensation for disturbances in the load voltages. It also aids to set up the desired voltage amplitude with appropriate period of compensation.

The control system consists of a reference signal generation technique and voltage controller. The reference signal generation technique is a new version of DQ method. The traditional DQ method has deficiency under unbalanced conditions. Similar to the traditional DQ method, the modified DQ method has phase locked loop (PLL) and Park transformation [26], [28]. A detection technique of positive sequence components and a peak finder technique are included in the modified DQ method. Algorithm of the technique is elaborated as follows.

A. DETECTION OF POSITIVE SEQUENCE COMPONENTS

The detected grid voltages during abnormal conditions have positive, negative and zero components as shown in Figure 5. The technique aims to separate three phasors that have equal magnitudes, displaced by 120° and rotate anticlockwise, which are the positive sequence components [50].

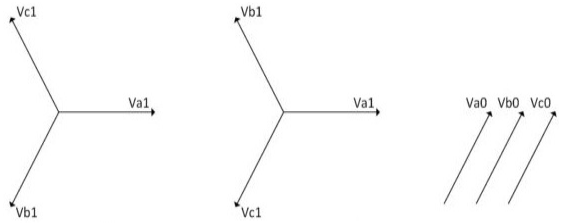

FIGURE 5. Symmetrical components of grid voltages.

As stated earlier, this technique is based on time domain. The time period is related to the phase angle as:

$$t_{dis} = \frac{\text{phase angle}}{360^\circ} \times \frac{1}{f} \tag{13}$$

where t_{dis} is the displacement period between two voltage phasors, f is the frequency. The symmetrical three-phase voltages of ungrounded system can be expressed as:

$$\mathbf{V_{abc}}(\mathbf{t}) = \begin{bmatrix} V_a \cos(\omega t + \theta) \\ V_b \cos\left(\omega t + \theta - \frac{2\pi}{3}\right) \\ V_c \cos\left(\omega t + \theta + \frac{2\pi}{3}\right) \end{bmatrix}$$

$$= V^{(1)} \begin{bmatrix} \cos\left(\omega t + \theta^{(1)}\right) \\ \cos\left(\omega t + \theta^{(1)} - \frac{2\pi}{3}\right) \\ \cos\left(\omega t + \theta^{(1)} + \frac{2\pi}{3}\right) \end{bmatrix}$$

$$+V^{(2)}\begin{bmatrix}\cos(\omega t+\theta^{(2)})\\ \cos(\omega t+\theta^{(2)}-\frac{2\pi}{3})\\ \cos(\omega t+\theta^{(2)}+\frac{2\pi}{3})\end{bmatrix} \quad (14)$$

The equation of symmetrical components is converted into time-domain to extract the positive sequence components as follow:

$$V^{(1)}_{(abc)}(t)=\begin{bmatrix}V^{(1)}_a(t)\\ V^{(1)}_b(t)\\ V^{(1)}_c(t)\end{bmatrix}=\begin{bmatrix}V^{(1)}(t)\\ V^{(1)}(T_\alpha)\\ V^{(1)}(T_\beta)\end{bmatrix} \quad (15)$$

$$V^{(1)}_{(t)}=\frac{1}{3}\left(\!\left(V_a(t)+V_b(T_\alpha)+V_c(T_\beta)\right)\!\right) \quad (16)$$

$$T_\alpha=\frac{240^\circ}{360^\circ}*\frac{1}{f}\quad T_\beta=\frac{120^\circ}{360^\circ}*\frac{1}{f} \quad (17)$$

where $V^{(1)}_{(t)}$ is the time domain representation of the positive sequence component for the three phase grid voltages, $t_{dis-\alpha}$ and $t_{dis-\beta}$ are the time phase shift of the symmetrical component. Where, $T_\alpha = t - t_{dis-\alpha}$ and $T_\beta = t - t_{dis-\beta}$. Figure 6 illustrate the extraction of grid voltage positive sequence component.

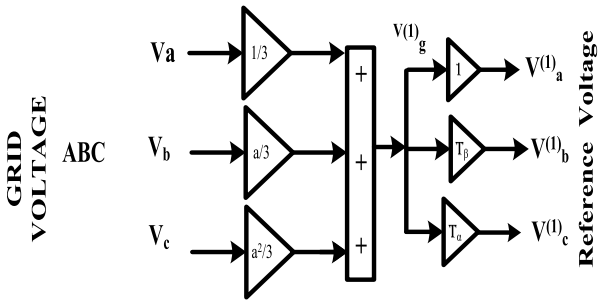

FIGURE 6. Extraction method of positive sequence components.

B. THE MODIFIED DQ TECHNIQUE

In the modified DQ technique a phase locked loop (PLL) is utilized to synchronize the signal to the grid fundamental voltage, $v^{(1)}_{g-abc}(t)$. Then the Park's transformation is used to transforms these voltage components to DC components (v_d, v_q) is derived in (18), as shown at the bottom of the next page.

To obtain the amplitudes of the reference signals at the desired voltage amplitude, peak finder is applied to $v^{(1)}_d$ as following

$$v^{(1)}_d=V^*_{desired}\frac{v^{(1)}_d}{v^{(1)}_d} \quad (19)$$

To transform the reference signal in abc coordinate system, inverse Parks transformation is applied as follow:

$$\mathbf{v_{L-abc,ref}}(\mathbf{t})=\begin{bmatrix}v_{La,ref}(t)\\ v_{Lb,ref}(t)\\ v_{Lc,ref}(t)\end{bmatrix}$$

$$=\sqrt{\frac{2}{3}}\begin{bmatrix}\cos(\omega t+\theta) & -\sin(\omega t+\theta)\\ \cos\left(\omega t+\theta-\frac{2\pi}{3}\right) & -\sin\left(\omega t+\theta-\frac{2\pi}{3}\right)\\ \cos\left(\omega t+\theta+\frac{2\pi}{3}\right) & -\sin\left(\omega t+\theta+\frac{2\pi}{3}\right)\end{bmatrix}\times\begin{bmatrix}v^{(1)}_d\\ v^{(1)}_q\end{bmatrix} \quad (20)$$

To explain the superiority of new DQ scheme compared to traditional DQ method, block diagrams for reference voltage generation in both schemes of new and traditional DQ are shown in figure 7 and 8 respectively. In modified DQ we can observe that the low pass filters are eliminated leading to less computation and fast response of the control system.

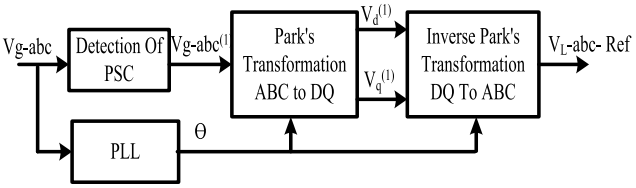

FIGURE 7. Modified DQ method.

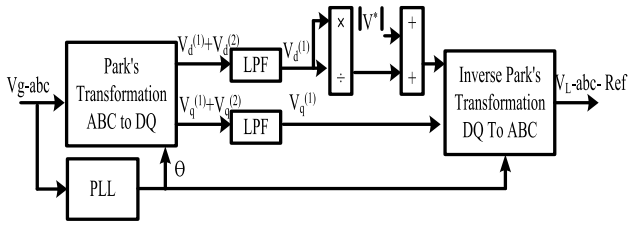

FIGURE 8. Traditional DQ method.

C. HYSTERESIS VOLTAGE CONTROLLER

A hysteresis voltage controller is applied to generate the switching signals for voltage source inverter. The hysteresis controller is preferred over traditional controllers like PWM, SVPWM because of its advantages of effective dynamic response, good accuracy, low cost and can be implemented easily [41]. The disadvantages of traditional techniques like switching losses with high switching frequency electromagnetic interference issues due to higher order harmonics, decrease in available voltage are overcome in the hysteresis control method [49], [51].

The generated voltage references are compared with the actual load voltages. The error between reference and actual voltage values are processed through the hysteresis band to produce the firing signals of inverter IGBT switches as shown in figure 9.

IV. EXPERIMENTAL SETUP

Figure 10 illustrates the experimental setup for the proposed DVR system. It consists of two circuits, a power circuit and

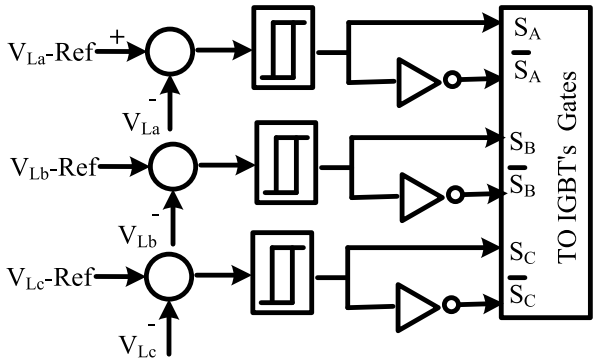

FIGURE 9. Hysteresis voltage controller.

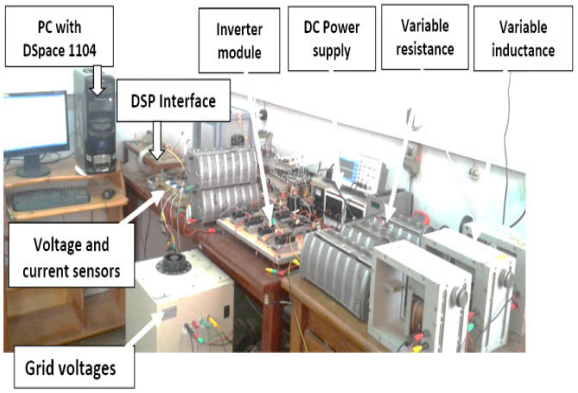

FIGURE 10. Experimental setup.

a control circuit. A three-phase AC voltage source, a transformer, VSI fed by a DC power supply and 1kVA load comprises the complete experimental circuit. The control circuit is based on employing dSPACE DS1104 control board. The supply and load voltages are measured using voltage sensors (LV25-P). To meet the criteria of the control board, voltage signals are scaled down to less than or equal to 10V.

TABLE 4. System parameters.

Parameters	Rating
Grid voltage	110 Vpeak
Fundamental frequency	50 Hz
Switching frequency	10 kHz
Load	P_{Load}=1 kW
Series transformer	1:1 ratio, 10 kVA
DC power supply	280 V
Lf, Cf, Rf	3 mH, 50 µF, 0.5 Ω

The system parameters are presented in Table 4.

V. RESULTS AND DISCUSSIONS

Series results at different scenarios of severe operation conditions are obtained to verify the validity of the proposed new schemes based on DQ technique as follow:

A. CASE 1: 20% BALANCED SAG

Under the condition of balanced 3Φ grid voltage with severe sag of 20%, figure 11 represents simulated results of the grid voltage having sag 20% from 0.8 second along with the load voltage and compensated voltage for traditional DQ control method, where the distortion in the load voltage wave is significantly observed. Simulated results of the balanced condition of 3Φ grid voltage with severe sag of 20% in the grid voltage from 0.8 second along with the load voltage and compensated voltage controlled by new version of DQ method are shown in figure 13, here the distortion in the load voltage wave is very less when compared to the traditional DQ method of control. It can be observed that the response on the control of the DQ is so fast that the instant of injecting compensation voltage is almost at the instant of 0.8 sec.

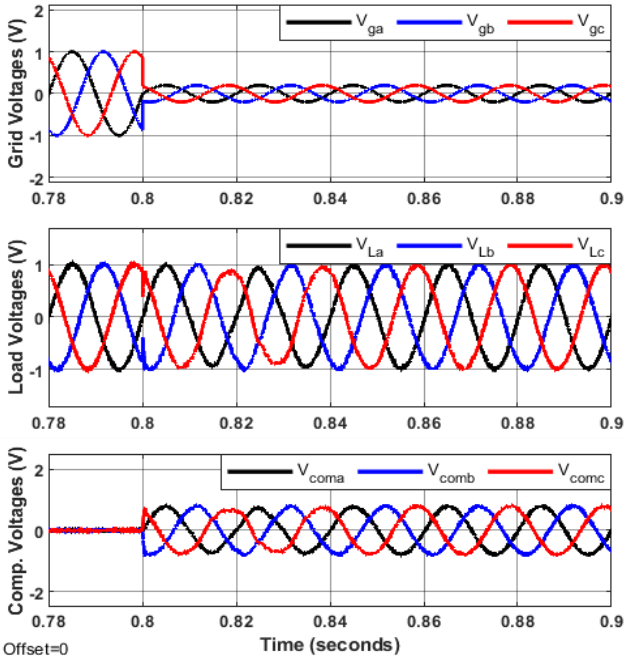

FIGURE 11. Simulation results of grid voltages, load voltage and DVR voltages (traditional DQ) under balanced 3φ grid voltage sag of 20%.

Figures 14 and 12 depict the experimental results of grid voltage, load voltage and compensated voltage with traditional DQ control and new version of DQ control respectively. In experimental method of new DQ the sag was initiated at 0.1 second and the compensated voltage was perfectly injected at the instant of 0.1 second. Both the experimental results of traditional and novel control are complimenting the simulated results.

$$\begin{bmatrix} v_d^{(1)} \\ v_q^{(1)} \end{bmatrix} = \sqrt{\frac{2}{3}} \begin{bmatrix} \cos(\omega t+\theta) & \cos\left(\omega t+\theta-\frac{2\pi}{3}\right) & \cos\left(\omega t+\theta+\frac{2\pi}{3}\right) \\ -\sin(\omega t+\theta) & -\sin\left(\omega t+\theta-\frac{2\pi}{3}\right) & -\sin\left(\omega t+\theta+\frac{2\pi}{3}\right) \end{bmatrix} \begin{bmatrix} v_{ga}^{(1)}(t) \\ v_{gb}^{(1)}(t) \\ v_{gc}^{(1)}(t) \end{bmatrix} \quad (18)$$

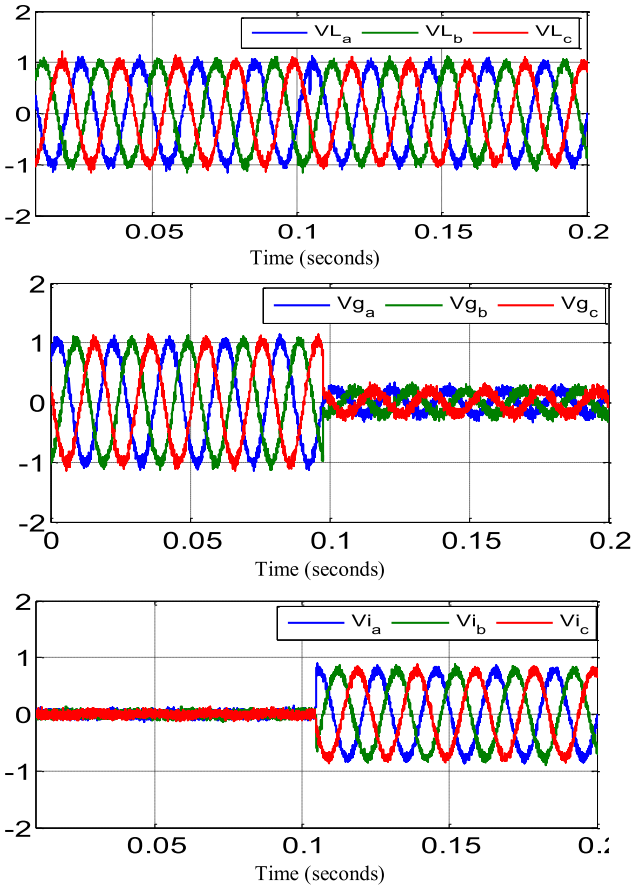

FIGURE 12. Experimental results of grid voltages, load voltage and DVR voltages (traditional DQ) under balanced 3φ grid voltage sag of 20%.

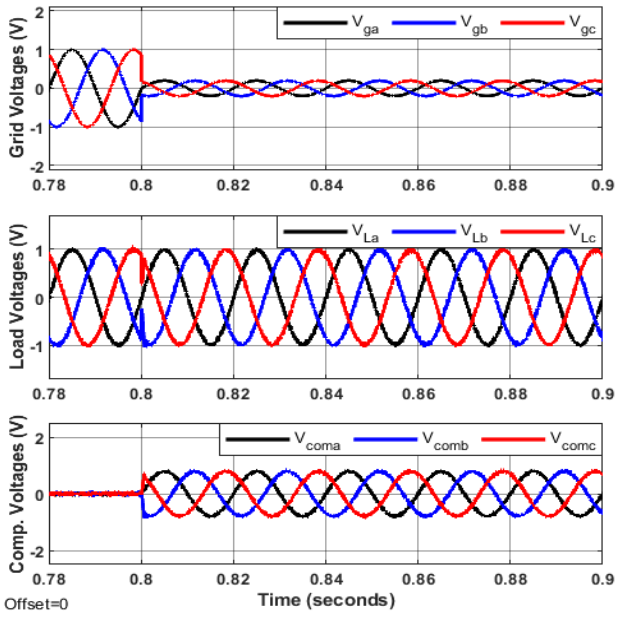

FIGURE 13. Simulation results of grid voltages, load voltage and DVR voltages (modified DQ) under balanced 3φ grid voltage sag of 20%.

Under the balanced condition with severe 20% voltage sag, the load voltage in per unit and load frequency for traditional and new DQ method are compared in Figure 15 under

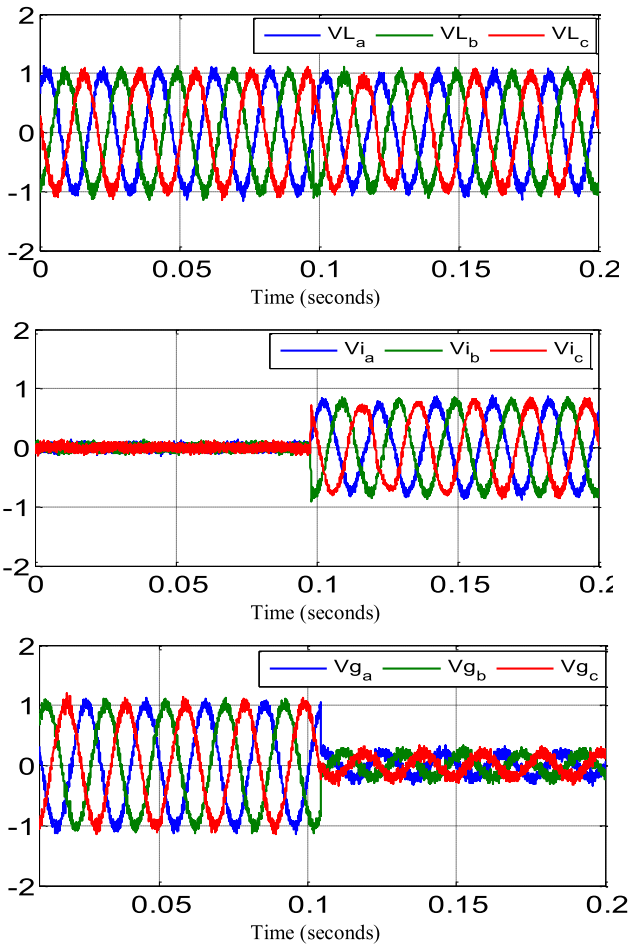

FIGURE 14. Experimental results of grid voltages, load voltage and DVR voltages (modified DQ) under balanced 3φ grid voltage sag of 20%.

a balanced scenario with 20% voltage sag. It shows, with tradition DQ, the voltage sags from 0.81 to 0.86 sec, with a maximum of 0.2 PU at 0.835 sec, whereas the load voltage is stable and no sag observed with the modified DQ method, indicating that the modified DQ controller is fast enough to identify the sag and compensate the sag voltage instantly. With the traditional DQ, load frequency fluctuation is detected during 0.8 sec to 0.97 sec, with a maximum change of 0.2 Hz at 0.875 sec. however, modified DQ technique has no significant variation in frequency from the nominal value of 50 Hz, indicating that the controller is effective in maintaining the stability of the system.

B. CASE 2: 70% BALANCED SWELL

For balanced 3 phase grid system another severe condition considered is 70% swell. Figure 16 depicts the simulation results of the grid voltage, load voltage and compensation voltage of a balanced three phase grid system with 70% severe swell. The swell in the grid is starting at 1.1 second and with the traditional DQ method the load voltage is still with distortions and slight swell in one or two phases

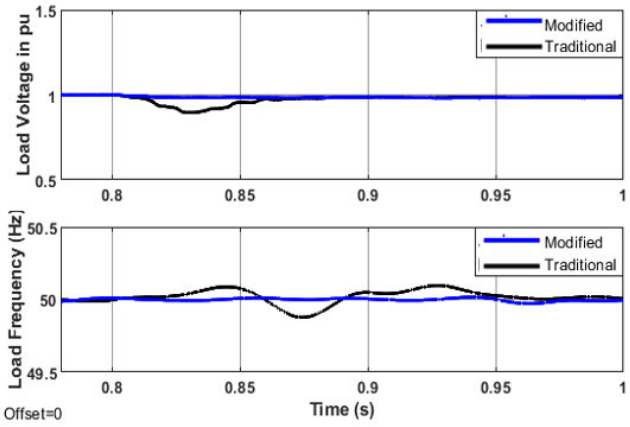

FIGURE 15. [Upper] pu load voltage, [Lower] load frequency under balanced 3φ grid voltage sag of 20%.

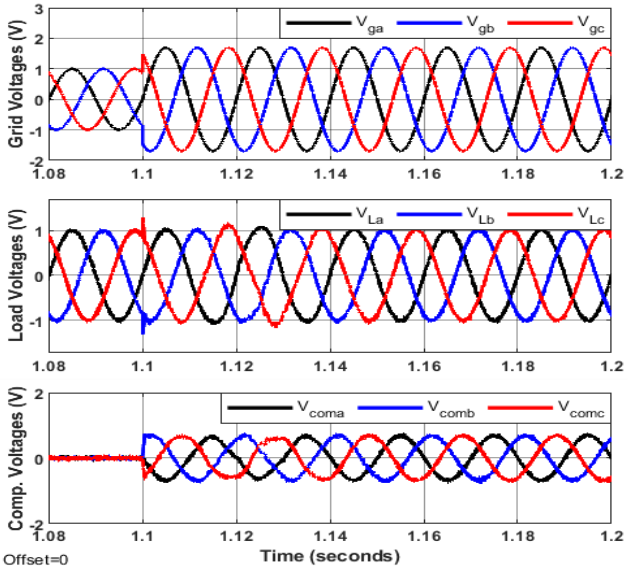

FIGURE 16. Simulation results of grid voltages, load voltage and DVR voltages (traditional DQ) under balanced 3φ grid voltage swell of 70%.

of load voltages as seen in Figure 16. Whereas, simulation results of grid voltage, load voltage and compensation voltage for severe 70% swell controlled by new DQ method are represented in Figure 18. With the novel DQ control the compensation voltage is initiated at exactly 1.1 second, more over the load voltage has shown a good voltage profile with less distortion and no swell sections in any of the phases.

Experimental results of three phase balanced grid voltage with 70% swell with traditional DQ control method are shown in Figure 19. in this experiment the swell is initiated at 0.075 second. The load voltage is displaying the effects of distortion and still some effect of swell is observed in some phases, as seen in the simulation results of traditional DQ control method. On contrary to the traditional DQ method the novel DQ method shows better voltage quality with low

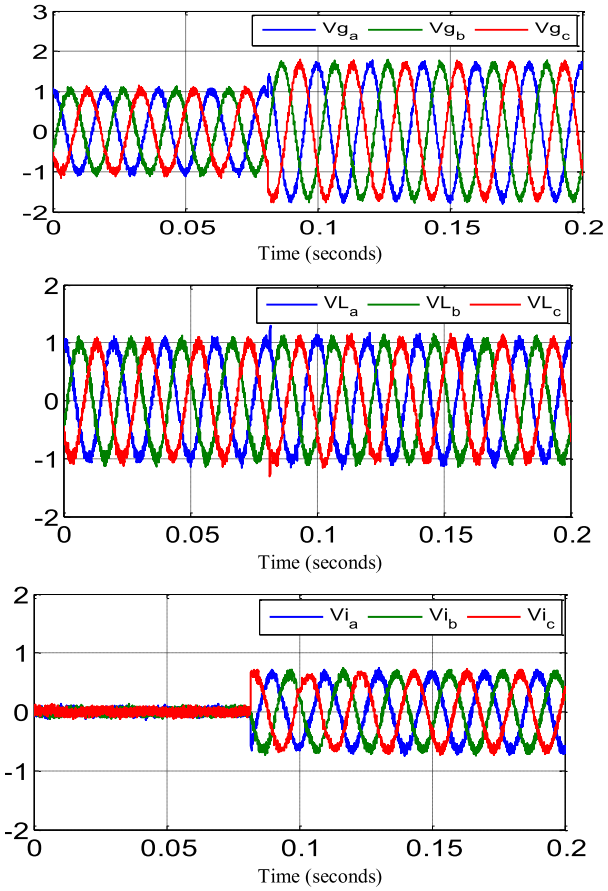

FIGURE 17. Experimental results of grid voltages, load voltage and DVR voltages (traditional DQ) under balanced 3φ grid voltage swell of 70%.

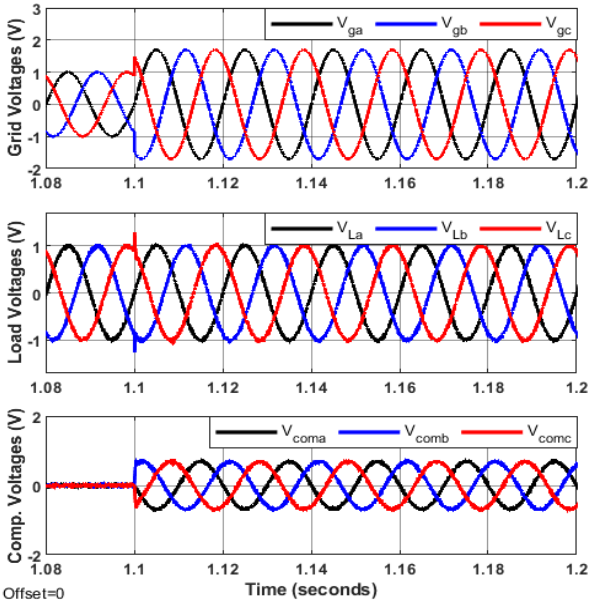

FIGURE 18. Simulation results of grid voltages, load voltage and DVR voltages (modified DQ) under balanced 3φ grid voltage swell of 70%.

distortions and no swell in the load voltage. The grid voltage, load voltage and compensation voltage for 70% swell conditions of a balanced three phase grid are represented in

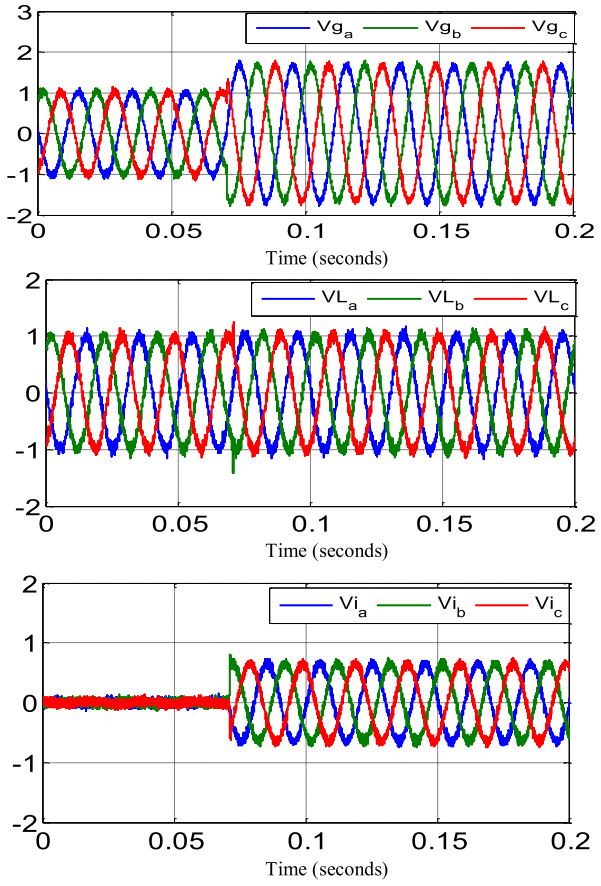

FIGURE 19. Experimental results of grid voltages, load voltage and DVR voltages (modified DQ) under balanced 3φ grid voltage swell of 70%.

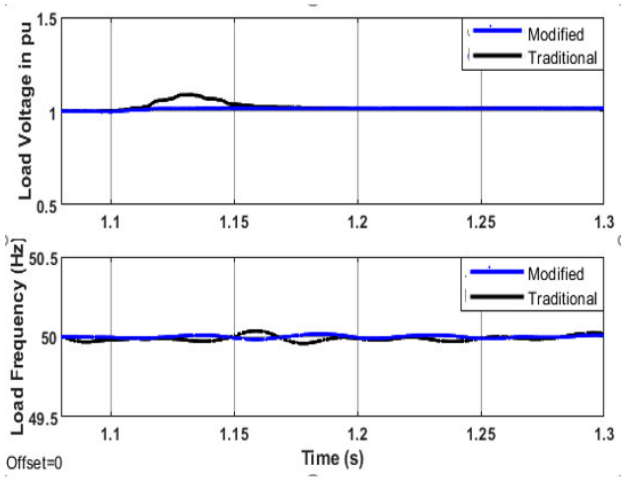

FIGURE 20. [Upper] pu load voltage, [Lower] lower load frequency under balanced 3φ grid voltage swell of 70%.

Figure 17. the compensated voltage is initiated exactly at the instant of 0.075 sec.

The per unit load voltage and load frequency of traditional and new DQ method are compared and displayed in Figure 20. The traditional DQ method has voltage swell from 1.12 sec to 1.15 sec, but with the modified DQ method the

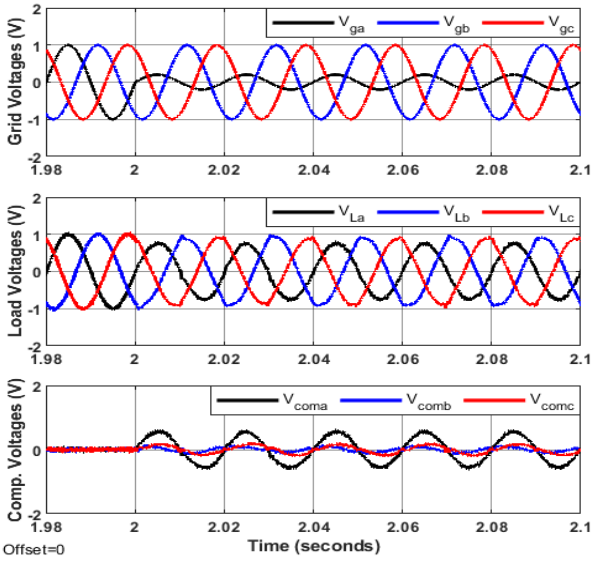

FIGURE 21. Simulation results of grid voltages, load voltage and DVR voltages (traditional DQ) under unbalanced 3φ grid voltage sag of 20%.

load voltage has shown stable characteristics with no swell. This means, the modified DQ has fast compensation response during the 70% balanced swell condition. For load frequency with traditional DQ, frequency change is observed during 1.1 to 1.25 sec with a maximum change of 0.175 Hz at 1.16 sec. On contrary, the proposed DQ method has shown a good control with maximum frequency variation of 0.05 Hz. New DQ has shown fast and effective control of the load frequency characteristics with balanced severe swell condition.

C. CASE 3: 20% UNBALANCED SAG

In this unbalanced case, one of the phases is affected with 20% sag. The simulation results of this unbalance condition with grid voltage, load voltage and compensation voltage with traditional DQ are shown in Figure 21. the sag in single phase is initiated at instant of 2 second because of which load voltage waveform is shown with distortion and the corresponding compensation voltage is injected at the same instant of sag initiation. When the proposed DQ control is implemented to compensate the 20% sag in one of the phase, the load voltage waveform shows less distortion and good profile of voltage. Simulated wave forms of Gird voltage, load voltage and corresponding compensation voltage with the proposed DQ control under 20% sag in one phase is presented in Figure 24. the compensation voltage under this unbalance condition is injected at the instant of 2 second.

Experiment result of traditional DQ control for unbalanced 20% sag condition is presented in Figure 22. On the other hand, the experimental result of new DQ control for 20% sag under unbalanced condition shows instantaneous injection of compensation voltage at 0.26 sec resulting in good quality of load voltage as shown in Figure 24.

Under condition of unbalance 20% sag the per unit load voltage and load frequency of traditional and new DQ method

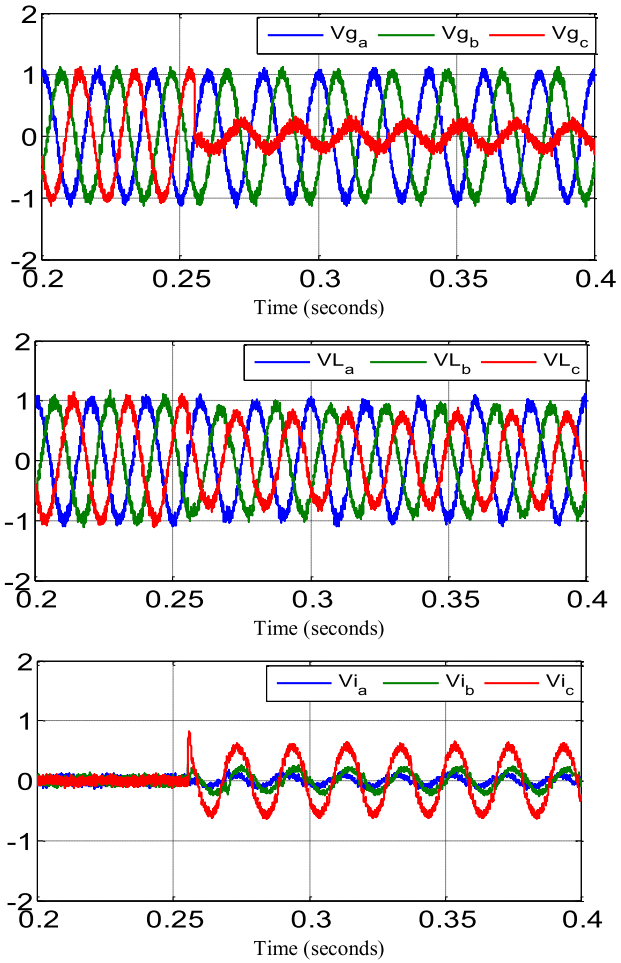

FIGURE 22. Experimental results of grid voltages, load voltage and DVR voltages (traditional DQ) under unbalanced 3φ grid voltage sag of 20%.

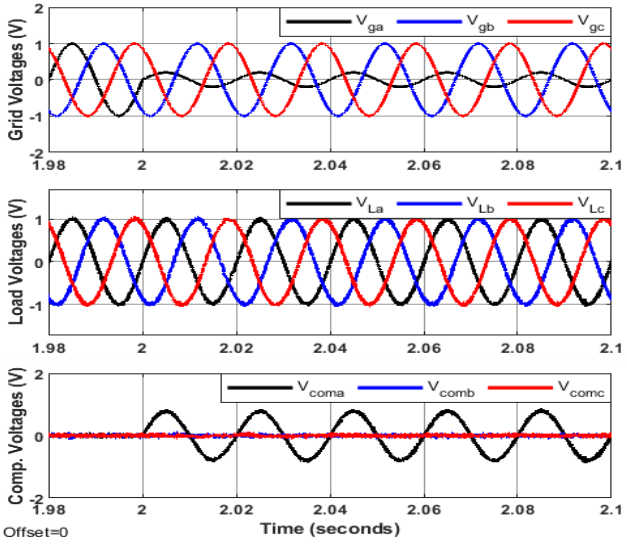

FIGURE 23. Simulation results of grid voltages, load voltage and DVR voltages (modified DQ) under unbalanced 3φ grid voltage sag of 20%.

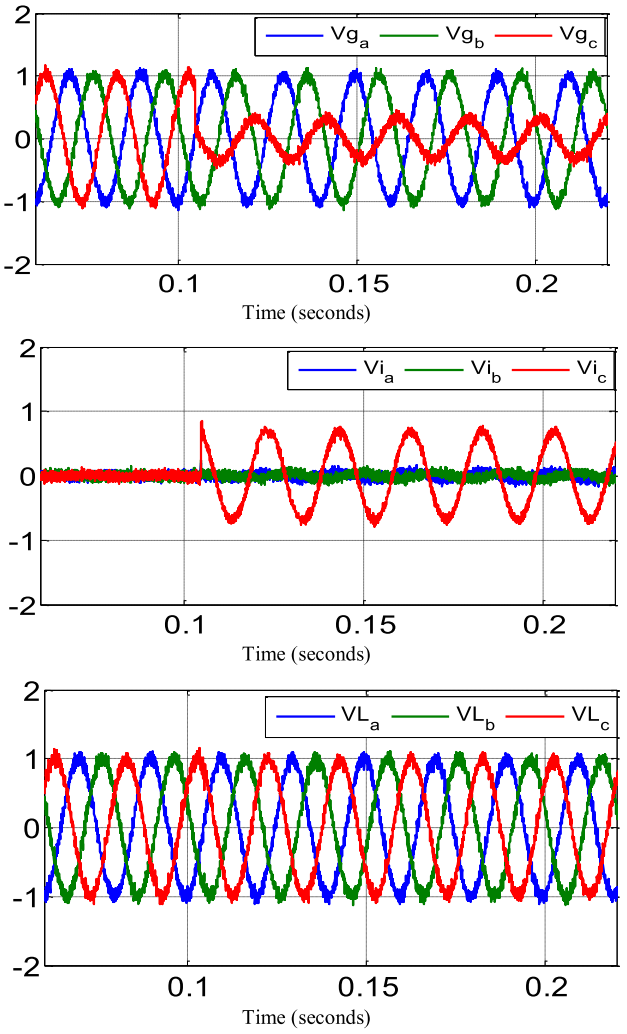

FIGURE 24. Experimental results of grid voltages, load voltage and DVR voltages (modified DQ) under unbalanced 3φ grid voltage sag of 20%.

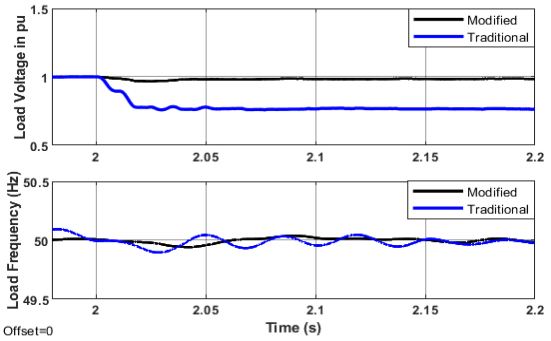

FIGURE 25. [Upper] pu load voltage, [lower] load frequency under balanced 3φ grid voltage sag of 80%.

are compared in Figure 25. With traditional DQ method, the load voltage has a sag of 0.2PU starting at 0.2 sec, whereas with the modified DQ method the load voltage has very low value of sag with less than 0.1 PU during 2.01 to 2.035 sec and recovered to the nominal value of 1 PU. This shows the efficacy and fast compensation of the proposed method. For load frequency with the traditional DQ, large fluctuations during 2 sec to 2.15 sec are observed with a maximum change

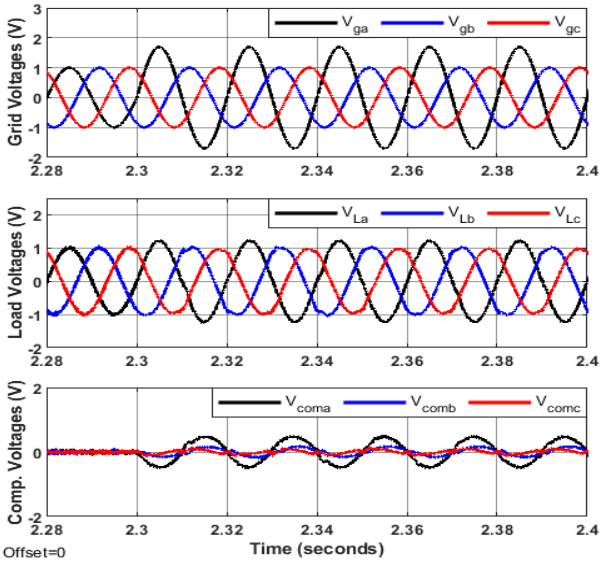

FIGURE 26. simulation results of grid voltages, load voltage and DVR voltages (traditional DQ) under unbalanced 3φ grid voltage swell of 70%.

of 0.15 Hz at 2.05 sec, with the Modified DQ technique the load frequency has shown very small fluctuations less than 0.075 Hz during 2 sec to 2.15 sec. This demonstrates the modified DQ technique's efficient control.

D. CASE 4: 70% UNBALANCED SWELL

Under the study of unbalanced condition with 70% swell in one of the phases, the simulated wave form of grid voltage, load voltage and compensation voltage with traditional DQ are presented in Figure 26 under this situation the load voltage have the severe distorted nature with one phase still exists with slight swell without complete compensation. On the other hand we can observe good compensation with new DQ method of control. The simulation results of grid voltage, load voltage and compensation voltage with new DQ method for unbalance 70% swell is shown in Figure 28.

Figure 27 shows the experimental results of unbalanced three phase grid with 70% swell with traditional DQ control method. Load voltage under this condition is having more distortion with swell still existing in the waveform. Figure 29 represents the experimental results of grid voltage, load voltage and compensated voltage injected at 0.11 sec. Under this new DQ control the load voltage has improved voltage profile with fully compensated swell.

With the condition of unbalance 70% swell the per unit load voltage and load frequency of traditional and new DQ method are compared in Figure 30. It explains, with traditional DQ method load voltage swell at 2.3 sec, with the change of 0.275PU. whereas with the modified DQ method for the load voltage swells the proposed DQ controller immediately responded to compensate the voltage to less than 0.1 PU during 2.3 to 2.34 sec. For load frequency with the traditional DQ, change in frequency is observed through 2.275 to 2.45 sec with a maximum change of 0.15 Hz at 2.3 sec. whereas, in Modified DQ method the load frequency

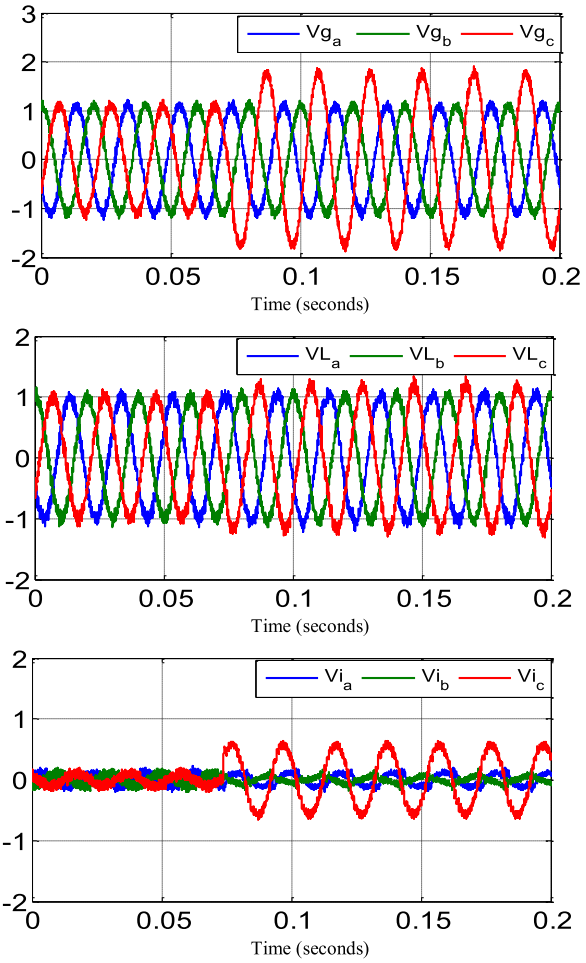

FIGURE 27. Experimental results of grid voltages, load voltage and DVR voltages (traditional DQ) under unbalanced 3φ grid voltage swell of 70%.

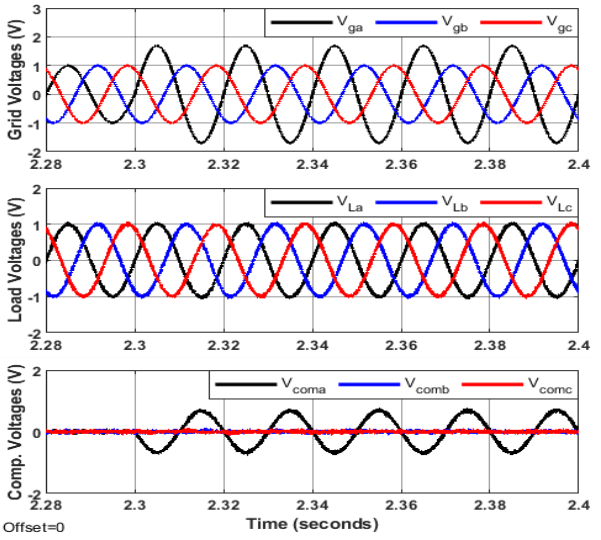

FIGURE 28. Simulation results of grid voltages, load voltage and DVR voltages (modified DQ) under unbalanced 3φ grid voltage swell of 70%.

change is less than 0.075 Hz during 2.275 to 2.45 Hz. This shows that the modified DQ has shown very fast attributes in detecting swell within a duration of 0.05 sec.

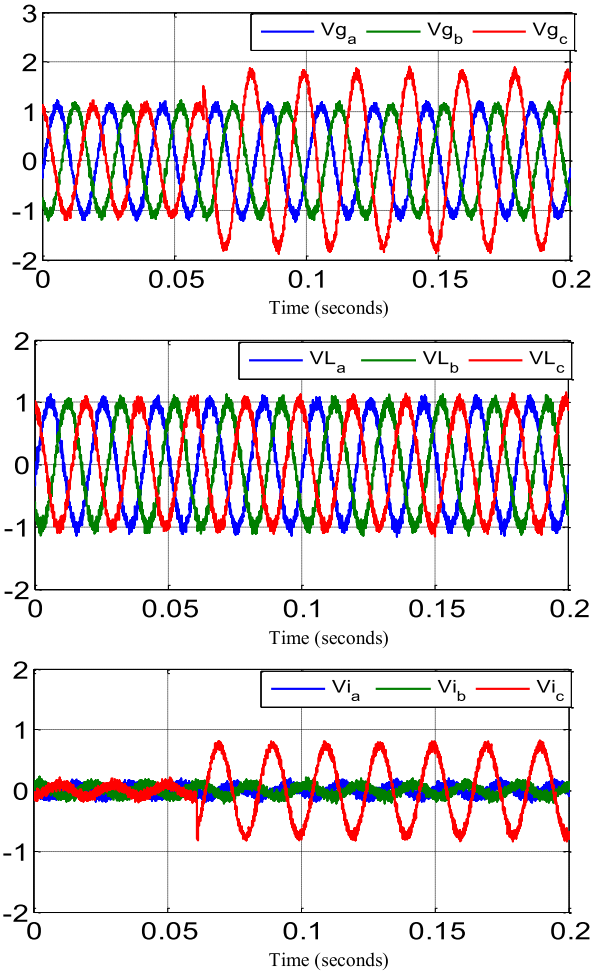

FIGURE 29. Experimental results of grid voltages, load voltage and DVR voltages (modified DQ) under unbalanced 3φ grid voltage swell of 70%.

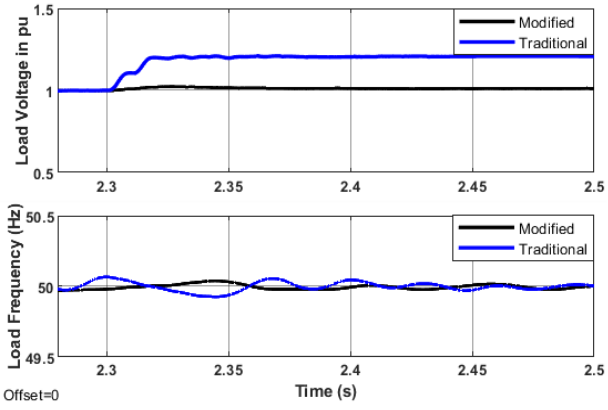

FIGURE 30. [Upper] pu load voltage, [lower] load frequency under balanced 3φ grid voltage swell of 70%.

From the results of both balanced and unbalanced three phase grid system with considered severe conditions of sag and swell, the experimental results validate the simulation result. The novel DQ control method shows good response in improving the voltage quality with less distortion in load voltage after the compensation.

VI. CONCLUSION

This paper inspects the control of DVR with modified DQ algorithm to generate reference voltage signals to control the DVR. The proposed DVR control method relies on a modified version of DQ theory with a detection method for the positive and negative sequence components. The modelled simulations are carried out in MATLAB Simulink and the results were validated with Experimental setup carried out on DSPACE 1104 module. The results are shown good correlation between simulation and experimental results.

The control of modified DQ method is compared with the traditional DQ control technique under the conditions of severe sag and swell. The performance of the controllers is also compared during balanced and unbalanced situation with severe cases of sag and swell. The comparative results suggest that the new modified DQ control method shows effective in compensating voltage during severe sag swell in balance and unbalance conditions with advantages of

- Less computational effort.
- Faster response.
- Less transient oscillation in the fundamental frequency under unbalanced voltage sag and swell.

REFERENCES

[1] S. Hasan, K. Muttaqi, D. Sutanto, and M. A. Rahman, "A novel dual slope delta modulation technique for a current source inverter based dynamic voltage restorer for mitigation of voltage sags," *IEEE Trans. Ind. Appl.*, vol. 57, no. 5, pp. 5437–5447, Sep. 2021, doi: 10.1109/TIA.2021.3089984.

[2] B. Bae, J. Jeong, J. Lee, and B. Hen, "Novel sag detection method for line-interactive dynamic voltage restorer," *IEEE Trans. Power Del.*, vol. 25, no. 2, pp. 1210–1211, Apr. 2010, doi: 10.1109/TPWRD.2009.2037520.

[3] M. Vilathgamuwa, A. A. D. Ranjith, S. S. Choi, and K. J. Tseng, "Control of energy optimized dynamic voltage restorer," in *Proc. IECON Conf. 25th Annu. Conf. IEEE Ind. Electron. Soc.*, vol. 3, Dec. 1999, pp. 873–878.

[4] P. Li, L. Xie, J. Han, S. Pang, and P. Li, "New decentralized control scheme for a dynamic voltage restorer based on the elliptical trajectory compensation," *IEEE Trans. Ind. Electron.*, vol. 64, no. 8, pp. 6484–6495, Aug. 2017, doi: 10.1109/TIE.2017.2682785.

[5] N. C. S. Sarita, S. S. Reddy, and P. Sujatha, "Control strategies for power quality enrichment in distribution network using UPQC," *Mater. Today, Proc.*, vol. 10, Feb. 2022, doi: 10.1016/j.matpr.2021.07.053.

[6] S. M. Deckmann and A. A. Ferrira, "About voltage sags and swells analysis," in *Proc. 10th Int. Conf. Harmon. Quality Power*, Oct. 2002, pp. 144–148, doi: 10.1109/ICHQP.2002.1221423.

[7] F. K. de Araújo Lima, J. M. Guerrero, F. L. Tofoli, C. G. C. Branco, and J. L. Dantas, "Fast and accurate voltage sag detection algorithm," *Int. J. Electr. Power Energy Syst.*, vol. 135, Feb. 2022, Art. no. 107516, doi: 10.1016/j.ijepes.2021.107516.

[8] Z. Elkady, N. Abdel-Rahim, A. A. Mansour, and F. M. Bendary, "Enhanced DVR control system based on the Harris hawks optimization algorithm," *IEEE Access*, vol. 8, pp. 177721–177733, 2020, doi: 10.1109/ACCESS.2020.3024733.

[9] *IEEE Recommended Practice for Monitoring Electric Power Quality*, Standard 1159-2019, IEEE Standards Association, 2019.

[10] M. I. Hossain, I. Rahaman, M. N. Rahman, M. F. Hasan, M. M. Hasan, and R. C. Sarker, "Voltage sag compensation in distribution system using dynamic voltage restorer," in *Proc. 2nd Int. Conf. Adv. Inf. Commun. Technol. (ICAICT)*, Nov. 2020, pp. 492–497, doi: 10.1109/ICAICT51780.2020.9333502.

[11] S. Zahra, M. Siddique, J. Hussain, S. Jabbar, and M. Riaz, "A new reliable single-stage single-phase AC–AC converter based dynamic voltage restorer for voltage sag/swell compensation," in *Proc. 3rd Int. Conf. Comput., Math. Eng. Technol. (iCoMET)*, Jan. 2020, pp. 1–11.

[12] M. Nagesh and N. S. Kodihalli, "Comparative analysis of performance of D-STATCOM and DVR for voltage sag, voltage swell and fault compensation," *Int. Res. J. Eng. Technol.*, vol. 5, no. 6, pp. 2884–2891, 2018.

[13] A. Pakharia and M. Gupta, "Dynamic voltage restorer for C ompensation of voltage sag and swell: A literature review," *Int. J. Adv. Eng. Technol.*, vol. 4, no. 1, pp. 347–355, 2012.

[14] Y. Jani, S. Savaliya, V. Solanki, and A. Mahavidyalaya, "A review on dynamic voltage restorer (DVR) to improve power quality," *Int. J. Eng. Sci. Res. Technol.*, vol. 3, no. 2, pp. 1–5, 2014.

[15] N. G. El Sayed, G. El-Saady, E.-N.-A. Ibrahim, and M. A. Mohamed, "Dynamic voltage restorer for enhancing distribution systems power quality," in *Proc. 7th Int. Japan–Africa Conf. Electron., Commun., Comput., (JAC-ECC)*, Dec. 2019, pp. 210–215, doi: 10.1109/JAC-ECC48896.2019.9051252.

[16] D. Szabo, R. Bodnar, M. Regul'a, and J. Altus, "Designing and modelling of a DVR in MATLAB," in *Proc. 15th Int. Sci. Conf. Electr. Power Eng. (EPE)*, May 2014, pp. 229–233, doi: 10.1109/EPE.2014.6839464.

[17] S. Suraya, S. M. Irshad, M. F. Azeem, S. F. Al-Gahtani, and M. H. Mahammad, "Multiple voltage disturbance compensation in distribution systems using DVR," *Eng., Technol. Appl. Sci. Res.*, vol. 10, no. 3, pp. 5732–5741, Jun. 2020, doi: 10.48084/etasr.3485.

[18] A. RAI and A. K. Nadir, "Modelling and & simulation of dynamic voltage resotorer DVR for enhancing voltage sag," *Sensors Transducers J.*, vol. 87, no. 1, pp. 85–93, 2008.

[19] S. N. Abdulazeez, D. Atilla, and C. Aydin, "Design of adaptive controller for regulating the voltage by a dynamic voltage restorer DVR," in *Proc. 2nd Int. Conf. Electr., Commun., Comput., Power Control Eng. (ICECCPCE)*, Feb. 2019, pp. 165–170, doi: 10.1109/ICECCPCE46549.2019.203767.

[20] H. H. Alhelou, M. Hamedani-Golshan, T. Njenda, and P. Siano, "A survey on power system blackout and cascading events: Research motivations and challenges," *Energies*, vol. 12, no. 4, p. 682, Feb. 2019, doi: 10.3390/en12040682.

[21] A. H. Soomro, A. S. Larik, M. A. Mahar, A. A. Sahito, A. M. Soomro, and G. S. Kaloi, "Dynamic voltage restorer—A comprehensive review," *Energy Rep.*, vol. 7, pp. 6786–6805, Nov. 2021, doi: 10.1016/j.egyr.2021.09.004.

[22] S. Jothibasu and M. K. Mishra, "A control scheme for storageless DVR based on characterization of voltage sags," *IEEE Trans. Power Del.*, vol. 29, no. 5, pp. 2261–2269, Oct. 2014, doi: 10.1109/TPWRD.2014.2316598.

[23] S. Suraya and K. S. R. Dr Anjaneyulu, "SRF controlled DVR for compensation of balanced and unbalanced voltage disturbances," *Int. J. Electr. Eng. Technol.*, vol. 7, no. 3, pp. 73–92, May 2016.

[24] R. E. Nambiar, D. M, L. B, P. K. Aj, and V. Priyadarshini, "Comparative study between different controllers of DVR for power quality improvement," in *Proc. Int. Conf. Design Innov. 3Cs Compute Communicate Control (ICDI3C)*, Jun. 2021, pp. 84–87, doi: 10.1109/ICDI3C53598.2021.00025.

[25] A. R. A. Jerin, P. Kaliannan, and U. Subramaniam, "Improved fault ride through capability of DFIG based wind turbines using synchronous reference frame control based dynamic voltage restorer," *ISA Trans.*, vol. 70, pp. 465–474, Sep. 2017, doi: 10.1016/j.isatra.2017.06.029.

[26] Q. E. Sahril, I. Sudiharto, and O. A. Qudsi, "A single phase dynamic voltage restorer (DVR) with direct AC–AC converter using dq transform to mitigate voltage sag," in *Proc. Int. Seminar Appl. Technol. Inf. Commun. (iSemantic)*, Sep. 2020, pp. 292–297, doi: 10.1109/iSemantic50169.2020.9234272.

[27] Q. Erfan Sahril, I. Sudiharto, and O. Asrarul Qudsi, "A single phase dynamic voltage restorer (DVR) with direct AC–AC converter using dq transform to mitigate voltage sag," in *Proc. Int. Seminar Appl. Technol. Inf. Commun. (iSemantic)*, Sep. 2020, pp. 292–297, doi: 10.1109/iSemantic50169.2020.9234272.

[28] H. Kaiming and F. Zhouxing, "Improved instantaneous derivation dq detection voltage drop method," in *Proc. IEEE 4th Adv. Inf. Technol., Electron. Autom. Control Conf. (IAEAC)*, Dec. 2019, pp. 2657–2662.

[29] J. Kim, J. Choi, and H. Hong, "Output LC filter design of voltage source inverter considering the performance of controller," in *Proc. PowerCon Int. Conf. Power Syst. Technol.*, vol. 3, Dec. 2000, pp. 1659–1664, doi: 10.1109/ICPST.2000.898225.

[30] A. Q. Jaelani, A. Rizqiawan, N. Hariyanto, and J. Choi, "DVR control based on stationary reference frame for unbalanced voltage sag compensation; DVR control based on stationary reference frame for unbalanced voltage sag compensation," in *Proc. IEEE Conf. Power Eng. Renew. Energy*, Oct. 2018, pp. 1–6.

[31] A. Karthikeyan, D. G. A. Krishna, A. Tejaswini, A. S. Panda, and R. L. Prasanna, "A comparative study of PI and PDF controllers for DVR under distorted grid conditions," in *Proc. 20th Nat. Power Syst. Conf. (NPSC)*, Dec. 2018, pp. 1–6.

[32] M. Farhadi-Kangarlu, E. Babaei, and F. Blaabjerg, "A comprehensive review of dynamic voltage restorers," *Int. J. Electr. Power Energy Syst.*, vol. 92, pp. 136–155, Nov. 2017, doi: 10.1016/j.ijepes.2017.04.013.

[33] N. G. El Sayed, G. El-Saady, E.-N.-A. Ibrahim, and M. A. Mohamed, "Dynamic voltage restorer for enhancing distribution systems power quality," in *Proc. 7th Int. Jpn.-Africa Conf. Electron., Commun., Computations, (JAC-ECC)*, Dec. 2019, pp. 210–215, doi: 10.1109/JAC-ECC48896.2019.9051252.

[34] V. K. Remya, P. Parthiban, V. Ansal, and A. Nandakumar, "Single-phase DVR with semi-Z-source inverter for power distribution network," *Arabian J. Sci. Eng.*, vol. 43, no. 6, pp. 3135–3149, 2018, doi: 10.1007/s13369-017-2841-3.

[35] M. Gonzalez, V. Cardenas, L. Moran, and J. Espinoza, "Selecting between linear and nonlinear control in a dynamic voltage restorer," in *Proc. IEEE Power Electron. Spec. Conf.*, vol. 4, no. 8, Jun. 2008, pp. 3867–3872.

[36] N. Abas, S. Dilshad, A. Khalid, M. S. Saleem, and N. Khan, "Power quality improvement using dynamic voltage restorer," *IEEE Access*, vol. 8, pp. 164325–164339, 2020, doi: 10.1109/ACCESS.2020.3022477.

[37] N. Abas, S. Dilshad, A. Khalid, M. S. Saleem, and N. Khan, "Power quality improvement using dynamic voltage restorer," *IEEE Access*, vol. 8, pp. 164325–164339, 2020, doi: 10.1109/ACCESS.2020.3022477.

[38] D. Danalakshmi, S. Prathiba, M. Ettappan, and D. M. Krishna, "Reparation of voltage disturbance using PR controller-based DVR in modern power systems," *Prod. Eng. Arch.*, vol. 27, no. 1, pp. 16–29, Mar. 2021, doi: 10.30657/pea.2021.27.3.

[39] R. Pal and S. Gupta, "Topologies and control strategies implicated in dynamic voltage restorer (DVR) for power quality improvement," *Iranian J. Sci. Technol., Trans. Electr. Eng.*, vol. 44, no. 2, pp. 581–603, Jun. 2020, doi: 10.1007/s40998-019-00287-3.

[40] J. Afonso, C. Couto, and J. Martins, "Active filters with control based on the p-q theory," *IEEE Ind. Electron. Soc.*, vol. 47, pp. 5–10, 2000. [Online]. Available: http://hdl.handle.net/1822/1921

[41] A. Moghassemi and S. Padmanaban, "Review dynamic voltage restorer (DVR): A ComprehensiveReview of topologies, power converters, Control methods, and modified configurations," *Energies*, vol. 13, pp. 1–35, Jan. 2020.

[42] L. Haichun, X. Lizhi, and X. Shaojun, "A new detection method of voltage sag based on period phase concept," in *Proc. 4th IEEE Conf. Ind. Electron. Appl.*, May 2009, pp. 3333–3337, doi: 10.1109/ICIEA.2009.5138820.

[43] M. Vilathgamuwa, A. A. D. R. Perera, S. S. Choi, and K. J. Tseng, "Control of energy optimized dynamic voltage restorer," in *Proc. IECON Ind. Electron. Conf.*, vol. 2, Nov. 1999, pp. 873–878, doi: 10.1109/IECON.1999.816526.

[44] P. Li, L. Xie, J. Han, S. Pang, and P. Li, "New decentralized control scheme for a dynamic voltage restorer based on the elliptical trajectory compensation," *IEEE Trans. Ind. Electron.*, vol. 64, no. 8, pp. 6484–6495, Aug. 2017, doi: 10.1109/TIE.2017.2682785.

[45] C. Zhan, "Dynamic voltage restorer with battery energy storage for voltage dip mitigation," in *Proc. 8th Int. Conf. Power Electron. Variable Speed Drives*, 2000, pp. 360–365, doi: 10.1049/cp:20000273.

[46] M. Engin, "Sizing and simulation of PV-wind hybrid power system," *Int. J. Photoenergy*, vol. 2013, pp. 1–10, Jan. 2013, doi: 10.1155/2013/217526.

[47] K. Hatua, A. K. Jain, D. Banerjee, and V. T. Ranganathan, "Active damping of output LC filter resonance for vector-controlled VSI-fed AC motor drives," *IEEE Trans. Ind. Electron.*, vol. 59, no. 1, pp. 334–342, Jan. 2012, doi: 10.1109/TIE.2011.2141093.

[48] G. A. de Almeida Carlos, C. B. Jacobina, J. P. R. A. Mello, and E. C. D. Santos, "Cascaded open-end winding transformer based DVR," *IEEE Trans. Ind. Appl.*, vol. 54, no. 2, pp. 1490–1501, Mar. 2018, doi: 10.1109/TIA.2017.2768531.

[49] M. Fatiha, M. Mohamed, and A.-A. Nadia, "New hysteresis control band of an unified power quality conditioner," *Electr. Power Syst. Res.*, vol. 81, no. 9, pp. 1743–1753, Sep. 2011, doi: 10.1016/j.epsr.2011.05.003.

[50] D. S. Pillai and N. Rajasekar, "A comprehensive review on protection challenges and fault diagnosis in PV systems," *Renew. Sustain. Energy Rev.*, vol. 91, pp. 18–40, Aug. 2018, doi: 10.1016/j.rser.2018.03.082.

[51] P. Thankachen and D. A. Thomas, "Hysteresis controller based fault current interruption using DVR," in *Proc. Annu. Int. Conf. Emerg. Res. Areas, Magn., Mach. Drives (AICERA/iCMMD)*, Jul. 2014, pp. 1–4.